Benchmark on neutron capture extracted from (d,p) reactions

A.M. Mukhamedzhanov,[1,*] F.M. Nunes,[2] and P. Mohr[3]

[1] *Cyclotron Institute, Texas A& M University, College Station, TX 77843, USA*
[2] *National Superconducting Cyclotron Laboratory and Department of Physics and Astronomy, Michigan State University, MI 48824, U.S.A.*
[3] *Strahlentherapie, Diakonie-Klinikum Schwäbisch Hall, D-74523 Schwäbisch Hall, Germany*

Direct neutron capture reactions play an important role in nuclear astrophysics and applied physics. Since for most unstable short-lived nuclei it is not possible to measure the (n,γ) cross sections, (d,p) reactions have been used as an alternative indirect tool. We analyze simultaneously ^{48}Ca$(d,p)^{49}$Ca at deuteron energies 2, 13, 19 and 56 MeV and the thermal (n,γ) reaction at 25 meV. We include results for the ground state and the first excited state of ^{49}Ca. From the low-energy (d,p) reaction, the neutron asymptotic normalization coefficient (ANC) is determined. Using this ANC, we extract the spectroscopic factor (SF) from the higher energy (d,p) data and the (n,γ) data. The SF obtained through the 56 MeV (d,p) data are less accurate but consistent with those from the thermal capture. We show that to have a similar dependence on the single particle parameters as in the (n,γ), the (d,p) reaction should be measured at 30 MeV.

PACS numbers: 21.10.Jx, 24.10.-i, 24.50.+g, 25.40.Hs

I. MOTIVATION

Reaction rates of capture reactions are a crucial input to astrophysical network calculations. In particular, neutron capture reactions, which play a pivotal role in the astrophysical r-process nucleosynthesis, have to be known for nuclei between the valley of β-stability and the neutron-drip line (see [1, 2, 3] and references therein). Typically the neutron capture rates for the r-process have been estimated using the statistical Hauser-Feshbach model, although this may be unreliable away from stability as the level density is low. (n,γ) cross sections for short-lived unstable nuclei cannot be measured experimentally and have to be taken from theory. However, the production of unstable nuclei close to the r-process path has become possible in the recent years, and neutron transfer experiments like (d,p) on these nuclei are becoming more and more feasible as beam intensity continues to rise. Experimental programs using such transfer reactions to derive (n,γ) rates (i.e. [4, 5, 6]) have shown promising results. Theoretical work is needed to place this indirect method on firmer grounds. Capture reactions can occur directly or through a resonance. This work focuses on the direct capture only and analyzes for the first time (d,p) and (n,γ) reactions simultaneously using the combination of spectroscopic factors (SF) and asymptotic normalization coefficients (ANC) [7, 8, 9]. In contrast to charged particle capture which is mostly peripheral (e.g. [10, 11]), neutron capture reactions may contain an important contribution from the nuclear interior and consequently be very sensitive to the spectroscopic factor of the final state [7, 8, 9]. One nucleon SFs were first introduced into nuclear physics in the context of the shell model, where a sequence of orbitals is generated by a mean-field. SFs provide a measure of the occupancy of these orbitals [12]. Even with modern residual interactions, shell model predictions appear to overestimate SFs for well bound systems when compared to experimental values [13, 14]. The cause for this disagreement is still not well understood and work along these lines is ongoing. SFs on unstable nuclei are usually extracted through reactions such as transfer or knockout [15]. Transfer reactions have been traditionally the prime method of spectroscopy in nuclear physics (see e.g. the recent compilation of (d,p) reactions [16]). In the standard analysis, the experimental cross section is compared with the predictions from the distorted wave Born approximation (DWBA) [17] or the adiabatic distorted wave approximation (ADWA) [18], and the SF is extracted from the normalization. At present, there is a large interest in (d,p) reactions, be it as an indirect measure of (n,γ) rates, as a testing ground for many-body structure models, or directly associated with stockpile issues [19]. In the conventional approach, the extracted SFs suffer from large uncertainty due to the ambiguity in the bound state and optical potential parameters. As example we note the recently measured (d,p) reactions on ^{82}Ge and ^{84}Se nuclei in inverse kinematics, which have been used to determine the neutron SFs of ^{83}Ge and ^{85}Se above the closed neutron shell at $N = 50$. These SFs were used to calculate the direct (n,γ) capture cross sections on ^{82}Ge and ^{84}Se [20]. However, the measured low-energy (d,p) reactions are peripheral; this leads to large uncertainties in the extracted SFs due to the ambiguity of the bound state potential parameters, which can deviate significantly from the standard ones for neutron-rich isotopes. For all these reasons, the methodology used when analysing (d,p) data has been recently revisited and questioned [7, 8]. As DWBA predictions are often the base for the extraction of the phenomenological SFs, sources of uncertainty in DWBA calculations need to be under control. Once one has ensured the validity of the

*Electronic address: akram@comp.tamu.edu

one-step approximation [21], one needs to assess the uncertainty in the optical potentials [22] and the bound state potential parameters [8]. Along these lines, a combined method of extracting SFs from transfer reactions, using the asymptotic normalization coefficients (ANCs) determined independently, was suggested and tested for different nuclei [7, 8, 9]. Introducing the ANC of the bound state in the formulation, one controls the normalization of the peripheral part of the reaction amplitude, generally a large contribution to the transfer cross section. This allows to significantly reduce the uncertainty in the choice of the bound state potential parameters and test the choice of the optical potential or the assumptions in DWBA. These same ideas can also be applied to direct capture reactions, breakup, and $(e, e'p)$. The ultimate goal of this work is to prove the principle that (d, p) reactions can indeed be used to extract (n, γ) rate, through a systematic methodology. Along these lines, an important step to validate the use of (d, p) reactions as an indirect tool to extract (n, γ) cross sections for exotic nuclei is to check for consistency between SFs extracted from (d, p) reactions and those from (n, γ) on stable nuclei, when there is a large variety of data to constrain the problem. We therefore benchmark the (d, p) method on ^{48}Ca$(n, \gamma)^{49}$Ca (ground state and first excited state). This choice is based on the very high quality data for thermal neutron capture, the well known neutron scattering length, and the number of (d, p) data sets on ^{48}Ca which all together present a stringent test for the applied reaction model. The paper is organized as follows. In section II, we provide some theoretical background and present the procedure used for extracting SFs from either (d, p) or neutron capture. In section III we include the details of the calculations and the data used, and present the results of our test case. Finally, in section IV we draw our conclusions.

II. THEORETICAL CONSIDERATIONS AND METHODOLOGY

In both $A(d, p)B$ and $A(n, \gamma)B$, the main nuclear structure input is the overlap function between the final state and the initial state $I^B_{An}(r)$, its norm being the SF. This many-body overlap function is usually approximated by a single particle state $\varphi_{An}(r)$ such that the many-body effects are hidden into the normalization factor:

$$I^B_{An}(r) = S^{1/2}\,\varphi_{An}(r). \quad (1)$$

Here, S is the neutron SF. We emphasize that Eq.(1) is an approximation, since the radial dependence of the overlap function and the nucleon bound state wave function can differ: the overlap function, as a many body object, includes, in addition to mean-field effects, the effects of residual interactions, which affect the nuclear surface region, the relevant region for direct reactions [23]. The single-particle function $\varphi_{An}(r)$ is the solution of the Schrödinger equation with a central potential, typically a Woods-Saxon potential of *standard* geometry. Asymptotically, the many-body overlap function and the single-particle function do have the same radial behaviour. Then, defining C as the asymptotic normalization coefficient of the overlap function, and b the single-particle asymptotic normalization coefficient, $C^2 = Sb^2$. It is clear that, if one knew b then knowing the ANC C would provide directly the SF S. However, this is hardly ever the case. Ambiguities in the single-particle parameters introduce ambiguities in the SF which are not well controlled [7, 8, 10]. The DWBA amplitude for the transfer reaction $A(d, p)B$ is given by $M^{dp} =< \psi^{(-)}_f \varphi_{An} | \Delta V | \varphi_{pn}\, \psi^{(+)}_i >$. The transition operator is written in post-form $\Delta V = V_{pn} + V_{pA} - U_{pB}$ with V_{ij} the interaction potential between i and j and U_{pB} the optical potential in the final-state. The distorted waves in the initial and final states are $\psi^{(+)}_i$ and $\psi^{(-)}_f$, and φ_{pn} is the deuteron wavefunction. Similarly, the reaction amplitude for the (n, γ) process in first order is given by $M^{n\gamma} =< \varphi_{An} | \hat{O} | \varphi^{(+)}_{scatt} >$, where $\hat{O}$ is the well known electromagnetic transition operator, and φ_{scatt} is the neutron incoming scattering wave, usually calculated with the same potential that generates the final neutron bound state φ_{An}. The amplitude for (n, γ) is given in the usual first order approximation and the operator is taken in the long-wavelength limit. The $A(d, p)B$ DWBA amplitude depends on the optical potentials in the initial and final states and the bound state potential, while the $A(n, \gamma)B$ reaction depends only on the V_{An} potential for the bound and scattering states. In either case, a phenomenological SF is typically extracted through normalizing the cross section to the corresponding data. As in [7, 8], and for illustration purposes only, one can split the total amplitude into an asymptotic part $M_{ext} = b\tilde{M}_{ext}$, corresponding to $r > R_N$ where the single-particle function already behaves as a Hankel function, and the remaining interior part M_{int}. The cross section is schematically given by

$$\sigma^\alpha \propto S\,|M^\alpha[b]|^2 = |S^{1/2}\,M^\alpha_{int}[b] + C\,\tilde{M}^\alpha_{ext}|^2, \quad (2)$$

where α stands for (d, p) or (n, γ). Here we express the dependence on the single particle parameters (r_0, a) by the single-particle ANC $b = b(r_0, a)$. Eq. (2) brings out important intuitive physics: the normalization of the external part of the reaction amplitude is governed by the ANC while the internal part is determined by the SF. If a reaction is completely peripheral, it is possible to extract the ANC from the normalization to the data without any single-particle ambiguity (i.e., no dependence on b). In general, there are contributions from both the internal and external region and it becomes important to fix the external part independently for an accurate determination of the SF. This is true for transfer and capture reactions. It is generally said that transfer reactions are surface peaked, however the internal/external relative contributions can change significantly with energy. For sub-Coulomb transfer reactions, one is only sensitive to

the asymptotic part of the neutron wavefunction, and the ANC can be extracted virtually without theoretical uncertainties. In [7, 8], the important realization was that, introducing this independent ANC into the formulation, one could then extract a SF from a transfer reaction at higher energy, reducing significantly the uncertainty from the single-particle parameters. Direct radiative capture (n,γ) can be mostly peripheral if there is a centrifugal barrier in the initial state (e.g. ^{14}C$(n,\gamma)^{15}$C [24]). However if there is no barrier at all ($s-$wave neutron capture), the interior contribution is important. At typical stellar energies of 10-300 keV, $s-$wave and $p-$wave capture cross sections are often comparable, see e.g. [25], so both the ANC and the SF are important ingredients to calculate the (n,γ) cross section. In this work we will analyse, en par, (d,p) reactions at several beam energies and the corresponding capture reaction on ^{48}Ca. By varying the single-particle radius within a reasonable interval and fixing the diffuseness, we generate a set of single-particle functions for a range of single-particle ANCs. For each of these, we calculate the (d,p) and (n,γ) cross sections. Normalizing the peak of the (d,p) angular distribution to the data at each energy, and normalizing the thermal neutron capture total cross section, we calculate phenomenological SFs. We choose (d,p) at sub-Coulomb energies, where the reaction is known to be peripheral, and normalize the theoretical cross section to the backward peak in the data. We include (d,p) at higher energies and normalize the theory to the first forward peak in the data. In this way we obtain a function $S^{dp}_{exp}(b)$ from each deuteron energy considered. We also extract $S^{n\gamma}_{exp}(b)$ from the thermal capture. These $S_{exp}(b)$ functions obviously vary differently with the single-particle ANC b. If there is consistency in the formulations, they should all intersect for a realistic b_0. This procedure is better illustrated by looking at the ANCs

$$[C^{dp}_{exp}(b)]^2 = S^{dp}_{exp}(b)\, b^2 \;\text{ and }\; [C^{n\gamma}_{exp}(b)]^2 = S^{n\gamma}_{exp}(b)\, b^2. \quad (3)$$

If the reaction is completely peripheral, $C_{exp}(b)$ is constant. If there is contribution from the interior, then $C_{exp}(b)$ has a slope. This slope will be more pronounced the larger the interior contribution. Our test case is ^{49}Ca, which is part of the r-process chart [1] and believed to be composed of the double magic ^{48}Ca core and a neutron single particle state, either $p_{3/2}$ for the ^{49}Ca ground state, or $p_{1/2}$ for the first excited state in ^{49}Ca. Direct capture is dominant for ^{48}Ca$(n,\gamma)^{49}$Ca because of the small reaction Q-value and the low level density (see Fig. 4 of [26]). These properties of the stable neutron-rich ^{48}Ca are close to the expected properties of nuclei close to the r-process path. For ^{48}Ca, direct neutron capture occurs via $s-$wave [26, 27, 28, 29] and has a significant contribution from the nuclear interior. Therefore it is an ideal test case since the result should be very sensitive to the ANC, but also to the SF. Another advantage of this choice is that the scattering length for $^{48}\mathrm{Ca}-n$ has been measured with sufficient accuracy $a = 0.356 \pm 0.088$ fm [30] which allows to determine the initial scattering potential V_{An} with very minor uncertainties [26]. Neutron radiative capture on ^{48}Ca [26, 27, 28, 29] and transfer ^{48}Ca$(d,p)^{49}$Ca [31, 32, 33] have been accurately measured at several beam energies, for both the ground state and the first excited state. Thermal (n,γ) data at 25 meV [26, 27] were measured with 6% accuracy, and sub-Coulomb (d,p) at 1.992 MeV [31] was measured with 10% accuracy. In this work we also use (d,p) data at 13 MeV and 19.3 MeV from [32] and at 56 MeV from [33].

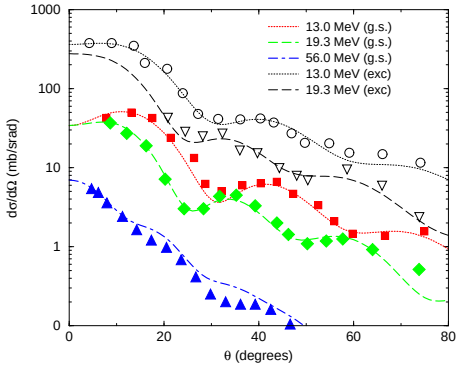

FIG. 1: (Color online) Angular distributions for ^{48}Ca$(d,p)^{49}$Ca compared to data populating the ground state: $E_d = 13$ MeV (red dotted line), $E_d = 19$ MeV (green dashed line) and $E_d = 56$ MeV (blue dot-dashed line). Also shown are the angular distributions to the first excited state: $E_d = 13$ MeV (black thin dotted line) and $E_d = 19$ MeV (black thin dashed line).

III. RESULTS

Neutron capture E1 cross sections are determined for the set of bound state wavefunctions corresponding to the single-particle radius within the range $r_0 = 1.05 - 1.65$ fm and fixed diffuseness $a = 0.65$ fm, with the Woods-Saxon depth V_{ws} adjusted to reproduce the correct binding energy of the final states in ^{49}Ca. The depth V_{ws} for the initial distorted wave is fixed to reproduce the $n - {}^{48}$Ca scattering length [30]. For the transfer calculations, following the procedure in [8], we use the Perey-Perey global optical potential [34] to define the optical potential in the exit channel and construct the deuteron potential in the entrance channel using ADWA [18], for all but the sub-Coulomb reaction (for the 1.99 MeV (d,p) calculations, we use the optical potentials presented in [31] although results are not sensitive to this choice – e.g. a variation of the potential depth by 10 % changes the reaction cross section by only about 1 %). ADWA includes deuteron breakup and thus goes well beyond one-step DWBA. The $n-^{48}$Ca and $p-^{48}$Ca potentials, needed to construct the finite range adiabatic deuteron potential [35], are also taken from [34]. ADWA is developed for reactions where the remnant $V_{pA} - U_{pB}$ can be neglected. We have checked that this is the case for ^{48}Ca(d,p). For V_{np} we use the Reid-soft-core [36]

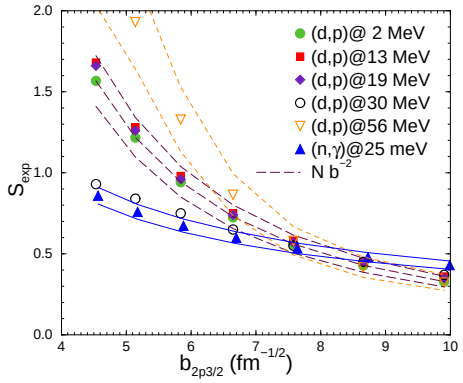

FIG. 2: (Color online) $S_{exp}(b)$ from ^{48}Ca$(d,p)^{49}$Ca$(g.s.)$ at $E_d = 1.99$ MeV (green dots), $E_d = 13$ MeV (red squares), $E_d = 19$ MeV (purple diamonds), $E_d = 30$ MeV (open circles) and $E_d = 56$ MeV (open triangles), and from ^{48}Ca$(n,\gamma)^{49}$Ca$(g.s.)$ at 25 meV (blue triangles). Also shown are the experimental uncertainties in the (d,p) reaction at 1.99 MeV (dashed lines), at 56 MeV (long-dashed lines) and the (n,γ) reaction (solid lines).

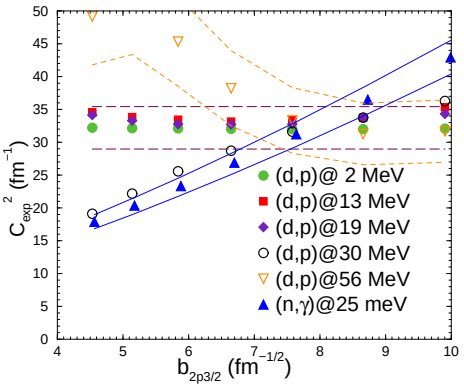

FIG. 3: (Color online) Same as Fig.2 but now referring to the ANC $C^2_{exp}(b)$. ANC and SF are related by Eq. (3).

although a simple Gaussian provides the same results. For the deuteron bound state we use [36] and for ^{49}Ca, the same set of bound state wavefunctions used for the (n,γ) calculations. All calculations are performed using FRESCO [37]. The shape of the angular distribution at 56 MeV [33], in particular in the forward angle region where it is most important, was not reproduced (this was also the finding in [16]). For that reason, instead of the Perey and Perey parameterization, we used the Koning and Delaroche [38] with which a significant improvement was obtained for the ground state. Calculated ADWA angular distributions are compared to the data in Fig.1. Results for the ^{49}Ca ground state are shown in Fig.2 and Fig.3 for $S_{exp}(b)$ and $C^2_{exp}(b)$ respectively. As expected, the sub-Coulomb (d,p) reaction is totally peripheral. At $E_d = 1.99$ MeV, the reaction is below the Coulomb barrier ($V_{CB} \approx 5$ MeV) both in the initial and final channels (Q-value is 2.924 MeV). $C^2_{exp}(b)$ remains constant over the broad interval of b: $C^2_{p_{3/2}} = 32.1 \pm 3.2$ fm^{-1} for the ^{49}Ca$(g.s.) \rightarrow {}^{48}$Ca $+ n$, see Fig.3. Consequently the SF behaves as $1/b^2$ as illustrated in Fig.2. The extracted ANC is insensitive to the optical and bound state potential parameters, the error bar coming from the systematic error of the data alone. At $E_d = 13$ and 19 MeV, the (d,p) reaction turns out to be also dominantly peripheral. It is reassuring that the $C^2_{exp}(b)$ extracted at these energies [32] are consistent with the sub-Coulomb result, corroborating the ADWA at these energies. However, we should note that, contrary to the 2 MeV case, these cross sections are sensitive to the choice of the optical potentials. The lack of b dependence makes it impossible to determine the SF from the 13 and 19 MeV data. Increasing the beam energy changes the picture. Fig.3 shows clearly that the 56 MeV data has a larger contribution from the interior and thus is more sensitive to the single particle parameters. Expectedly, as the single particle ANC increases, so does the external contribution, which explains the flattening of the $C^2(b)$ curve from the 56 MeV (d,p) data. The error band is represented by the long-dashed lines in Figs.2 and 3. The cross sections at this energy were measured with 10% accuracy but we have added in quadrature another 10% due to the dependence on the optical potentials. From the joint analysis of the 2 MeV data and the 56 MeV data, we can extract a spectroscopic factor $S_{exp} = 0.55 \pm 0.25$. The results for the ANC extracted from ^{48}Ca$(n,\gamma)^{49}$Ca$(g.s.)$ show a strong b dependence, in perfect agreement with [39], confirming an important contribution from the nuclear interior. From the overlapping regions in Fig.3, we obtain $b_0 = 7.80 \pm 1.2$ fm$^{-1/2}$ and $S_{exp} = 0.53 \pm 0.11$, in agreement with the value obtained from the 56 MeV transfer data. This $b_0 = 7.80$ fm$^{-1/2}$ corresponds to $r_0 \approx 1.45$ fm, a radius larger than the standard value. The determined SF is lower than one could expect from the independent particle shell model, confirming the reduction of the SF previously seen [14], and now the ambiguity of the bound state potential parameters has been eliminated. One may ask whether there are deuteron energies $20 < E_d < 56$ (MeV) for which the (d,p) cross sections show the same sensitivity to the nuclear interior as the corresponding (n,γ). We find that $E_d = 30$ MeV provides an excellent match. ADWA is expected to perform well in this energy region, as the adiabatic condition is satisfied (see [22] for a successful application on ^{12}C). We thus consider the (d,p) reaction at $E_d = 30$ MeV and apply an arbitrary normalization to the cross section (open circles in Fig.2 and Fig.3). Clearly illustrated in Fig.3, $C^2_{exp}(b)$ obtained from the (d,p) reaction at 30 MeV has a similar b dependence as the $C^2_{exp}(b)$ from the (n,γ) process. We emphasize that a (d,p) experiment on ^{48}Ca at this energy would be very useful; plans for such an experiment have been initiated by the present study [40]. We also study the (d,p) and (n,γ) reactions to the first excited state in ^{49}Ca. Results for $S_{exp}(b)$ and $C^2_{exp}(b)$ show the same pattern as for the ground state. Because of the relation between ANC and SF we show only $C^2_{exp}(b)$

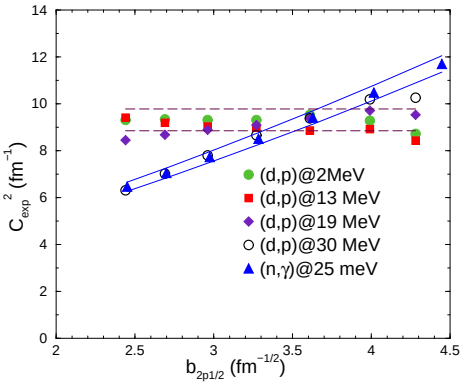

FIG. 4: (Color online) Same as Fig.3 but now referring to first excited state in ^{49}Ca.

in Fig.4. We obtain from sub-Coulomb (d,p) reaction, $C^2_{p_{1/2}} = 9.30 \pm 0.93$ fm^{-1}. Reactions at 13 and 19 MeV remain peripheral and the 56 MeV distribution is not well described by our model. Again, the (d,p) at 30 MeV and the (n,γ) show a similar sensitivity to the interior as for the ground state transition. Our sub-Coulomb (d,p) and (n,γ) joint analysis provides $b_0 = 3.63^{+0.54}_{-0.58}$ fm$^{-1/2}$ and $S_{exp} = 0.71^{+0.20}_{-0.12}$. Again, this b_0 corresponds to $r_0 \approx 1.45$ fm, showing consistency in the geometry of the neutron $p_{3/2}$ and $p_{1/2}$ orbitals. The large radii r_0 give further evidence for a neutron skin in neutron-rich calcium isotopes [41].

IV. CONCLUSIONS

Our goal was to provide a proof of principle that (d,p) reactions can indeed be used to extract (n,γ) rates, through a systematic methodology. As sub-Coulomb or near-Coulomb-barrier (d,p) reactions are peripheral, they provide an ANC virtually free from optical potential ambiguities. Whenever the (n,γ) reaction is peripheral, this is the only necessary bound state information needed for calculating the neutron capture cross section at low energy. If the (n,γ) is not peripheral, one needs to know both, the ANC and the SF. We have shown for ^{48}Ca that SFs obtained from thermal capture and 56 MeV (d,p) are consistent. Our results suggest that (d,p) data at energies around $E_d = 30$ MeV has a similar interior contribution as the (n,γ) and could thus be a better tool for extracting the (n,γ) cross sections. In order to confirm this, experiments at 30 MeV providing cross sections with better than 10% accuracy, would be very useful. Any prediction of neutron capture cross sections on unstable nuclei will be complicated by the fact that the neutron scattering length will not be measurable in most cases. This leads to an additional uncertainty because the scattering potential is not as well-defined as for the presented example $^{48}\mathrm{Ca} - n$. A rough estimate (see e.g. Fig. 5 of Ref. [26]) shows that this additional uncertainty remains below a factor of two for realistic variations of the neutron scattering potential. A detailed study of uncertainties of neutron capture cross sections for unstable nuclei will be given in a forthcoming paper.

From this work, we also find that $s-$wave (n,γ) reactions are actually very well suited for extracting a SF. For the (n,γ) process, the transition operator is well known, the ambiguity in the optical potential at very low energies is negligible when imposing the correct neutron scattering length, and the ambiguity of the bound state potential parameters is greatly reduced by fixing the asymptotic part of the bound state, say through sub-Coulomb reactions. Hence, the joint analysis of low energy (d,p) and thermal $s-$wave (n,γ) provides a powerful method to test microscopic structure models. This work is supported by the NNSA-DOE Grants DE-FG02-93ER40773 and DE-FG52-03NA00143 with a Rutgers subcontract DE-FG52-06NA26207, and the National Science Foundation, under grant PHY-0555893.

[1] S. Goriely, Astron. Astrophys. **325**, 414 (1997).
[2] M. Arnould, S. Goriely, and K. Takahashi, Phys. Rep. **450**, 97 (2007).
[3] F.-K. Thielemann *et al.*, Prog. Part. Nucl. Phys. **46**, 5 (2001).
[4] K.L. Jones *et al.*, Phys. Rev. C 70, 067602 (2004).
[5] J.S. Thomas *et al.*, Phys. Rev. C 71, 021302 (2005).
[6] J.S. Thomas *et al.*, Phys. Rev. C 76, 044302 (2007).
[7] A. M. Mukhamedzhanov and F. M. Nunes, Phys. Rev. C **72**, 017602 (2005).
[8] D. Y. Pang, F. M. Nunes, A. M. Mukhamedzhanov, Phys. Rev. C **75**, 024601 (2007).
[9] S. A. Goncharov *et al.*, Sov. J. Nucl. Phys. **35**, 383 (1982).
[10] H. M. Xu *et al.*, Phys. Rev. Lett. **73**, 2027 (1994).
[11] P. F. Bertone *et al.*, Phys. Rev. C **66**, 055804 (2002).
[12] B.A. Brown and B.H. Wildenthal, Annu. Rev. Nucl. Part. Sci. 38, 29 (1988).
[13] B.A. Brown *et al.*, Phys. Rev. C **65**, 061601(R) (2002).
[14] Jenny Lee *et al.*, Phys. Rev. C **73**, 044608 (2006).
[15] J. Al-Khalili and F. Nunes, J. Phys. G **29**, R89 (2003).
[16] Jenny Lee, M. B. Tsang, and W. G. Lynch, Phys. Rev. C **75**, 064320 (2007).
[17] N. Austern, Direct Nuclear Reaction Theories (Wiley, New York, 1970).
[18] R.C. Johnson, AIP Conf. Proc. **791**, 132 (2005).
[19] J. Cizewski, Fall meeting of the Division of Nuclear Physics APS (2006).
[20] J. S. Thomas *et al.*, Phys. Rev. **C 76**, 044302 (2007).
[21] F. Delaunay, F. M. Nunes, W. G. Lynch, and M. B. Tsang, Phys. Rev. C 72, 014610 (2005).
[22] X.D. Liu *et al.*, Phys. Rev. C 69 (2004) 064313.
[23] G. M. McAllen, W. T. Pinkston and G. R. Satchler, Particles and Nuclei **1**, 412 (1971).
[24] N. K. Timofeyuk *et al.*, Phys. Rev. Lett. **96**, 162501

(2006).
[25] P. Mohr *et al.*, Phys. Rev. C **58**, 932 (1998).
[26] H. Beer *et al.*, Phys. Rev. C **54**, 2014 (1996).
[27] F. P. Cranston and D. H. White, Nucl. Phys. **A169**, 95 (1971).
[28] P. Mohr *et al.*, Phys. Rev. C **56**, 1154 (1997).
[29] F. Käppeler, G. Walter, and G. J. Mathews, Astrophys. J. **291**, 319 (1985).
[30] V.F. Sears, Neutron News **3**, 26 (1992).
[31] J. Rapaport, A. Sperduto and M. Salomaa, Nucl. Phys. **A197**, 337 (1972).
[32] W. D. Metz *et al.*, Phys. Rev. C **12**, 827 (1975).
[33] Y. Uozumi *et al.*, Nucl. Phys. **A576**, 123 (1994).
[34] C. M. Perey and F. G. Perey, At. Data Nucl. Data Tables **17**, 1 (1976).
[35] G. L. Wales and R. C. Johnson, Nucl. Phys. **A274**, 168 (1976).
[36] V. Reid, Ann. Phys. (N.Y.) **50**, 411 (1968).
[37] I. J. Thompson, Comput. Phys. Rep. **7**, 167 (1988).
[38] A.J. Koning and J.P. Delaroche, Nucl. Phys. **A713**, 231 (2003).
[39] D. Baye, Phys. Rev. C **70**, 015801 (2004).
[40] R.E. Tribble, *private communication.*
[41] C. A. Bertulani, J. Phys. G **34**, 315 (2007).